

# High Density Xenon gas TPC for double beta decay search

- References are from “Noble Gas Detectors” unless otherwise noted.

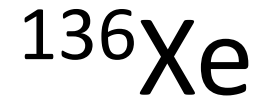
# Baseline design

- 1 ton enriched  $^{136}\text{Xe}$  gas (not liquid)
- At 15~30 times higher density than STP
  - $\rho = 0.088\sim 0.18\text{g/cm}^3$
  - e.g.  $\phi 2\text{m}\times 1.7\text{m(H)}$  cylinder at  $0.18\text{g/cm}^3$
- Use ionization (either at ionization or proportional mode) for energy measurement
  - Energy resolution goal  $< 0.5\%$ (FWHM)
- Tracking as TPC
  - Range(2.5MeV e)  $\sim 210\text{cm}$  at STP
  - $T_0$  by primary scintillation signal
  - Sample 15~20 points using pads (not wire).  $\sim 5\text{mm}$  spacing.
  - Purpose is to identify two blobs at track ends.  $\rightarrow$  distinguish from  $\alpha$ 's and  $\gamma$ 's.

# Double Beta decay candidates

	abound(%)	$\tau(2\nu\beta\beta)$ yr	Q(keV)	$Q^5/1E16$	$Q^5 \times \tau(2\nu\beta\beta)/1E36$	
48Ca	0.187	3.9E+19	4271	142.12	55.4	enrichment difficult
76Ge	7.8	1.7E+21	2039	3.52	59.9	
82Se	9.2	9.6E+19	2995	24.10	<b>23.1</b>	
96Zr	2.8	2.0E+19	3350	42.19	8.4	
100Mo	9.6	7.1E+18	3034	25.71	<b>1.8</b>	
110Pd	11.8		2013	3.31		
116Cd	7.5	2.8E+19	2802	17.27	4.8	
124Sn	5.64		2228	5.49		
130Te	34.5	7.6E+20	2529	10.35	78.6	
136Xe	8.9	2.2E+21	2479	9.36	<b>208.8</b>	
150Nd	5.6	9.2E+18	3367	43.27	4.0	enrichment difficult

\*  $\tau(2\nu\beta\beta) \propto Q^{11}$ ,  $\tau(0\nu\beta\beta) \propto Q^5$



- Xenon production rate
  - 5000-7000m<sup>3</sup>/yr ~50ton in 1998.
- 2x10<sup>6</sup> kton exists in air
- Enrichment is relatively easy.

	Density at 0°C,1atm (g/L)	Liquid Density (g/cm <sup>3</sup> )	Melting point(K)	Boiling point(K)
He	0.1786	0.145	-	4.22
Ne	0.9002	1.2	24.56	27.07
Ar	1.784	1.398	88.80	87.30
Kr	3.749	2.413	115.79	119.93
Xe	5.894	3.053	161.4	165.03

# Energy resolution

- Statistical limit
  - W-value 21.5 eV, Fano factor  $< 0.17 \rightarrow 0.29\%$  (FWHM)
- At higher density, energy resolution becomes worse.  $\rightarrow$  reject liquid option.

*A. Bolotnikov, B. Ramsey / Nucl. Instr. and Meth. in Phys. Res. A 396 (1997) 360–370*

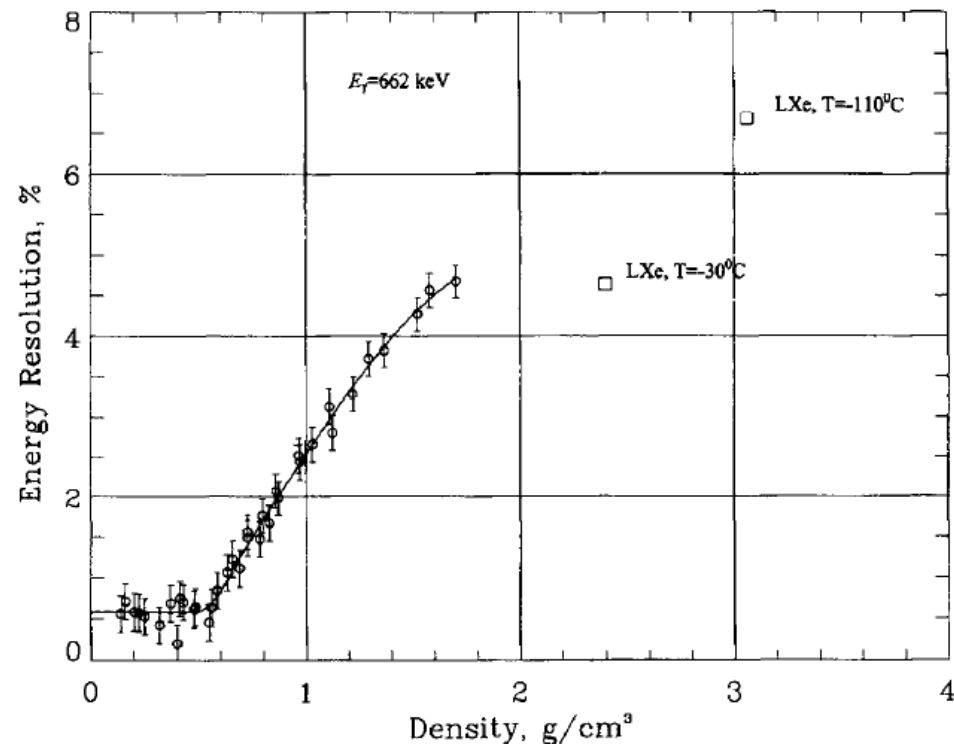
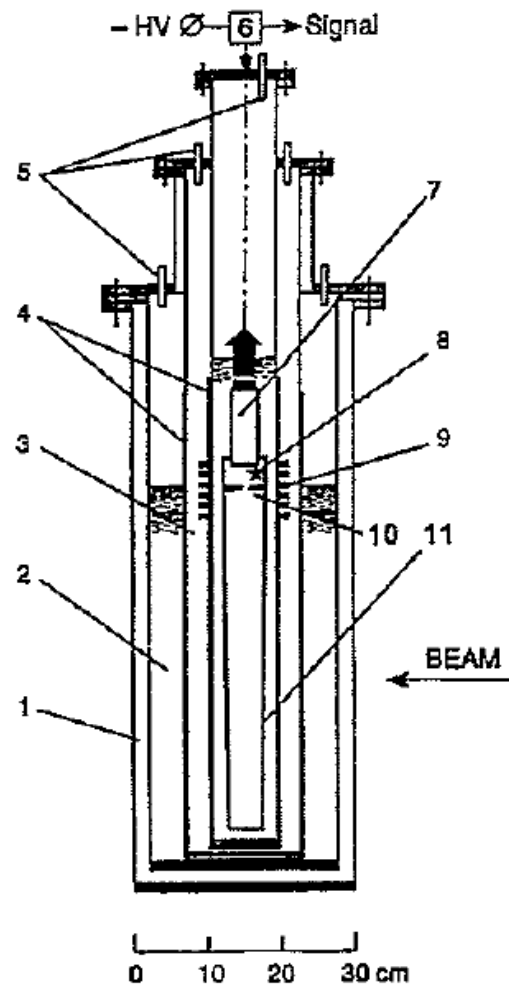


Fig. 5. Density dependencies of the intrinsic energy resolution (%FWHM) measured for 662 keV gamma-rays.

# High density (15~30 x STP)

Two options

- High pressure
  - Need pressure vessel including feed through
  - Need photo detector operatable at high pressure
  - Do not need cryo-system
- Low temperature at 1 atm.
  - $T = (273-165)/n+165 \text{ K}$  (Is this correct?)
    - $n=15\sim30$  (density in unit of STP state)
    - Boiling point 165.0K
    - 172.2K for  $n=15$ , 168.6 K for  $n=30$
  - Need cryo-system
    - In case of ionization mode operation, anyway preamprefiers need to be cooled.
  - Do not need pressure vessel feed through
  - PMT available
- Is characteristic same for these two?



冷却オプションだとこんな感じ？  
 (この例は、液体Xeだけれど、ガスでも使える?)

**Fig. 4.8** Detector CRISA, used for measurements of scintillation in LXe, LKr, and their mixtures excited by relativistic particles at ITEP accelerator. 1 - vacuum cryostat, 2 - liquid nitrogen jacket, 3 - nitrogen gas jacket, 4 - copper screens, 5 - gas inlets, 6 - PMT base, 7 - 30-mm diameter FEU-85 photomultiplier with p-terphenyl coated glass window, 8 - reference alpha source, 9 - heater, 10 - optical diaphragm, 11 - optical cell with UV light absorbing walls [182].



# Electric Field and drift velocity

## Drift velocity

- 1.05m/ms @ 'normal condition' w/  
 $E/N=0.303E-17$  V/cm<sup>2</sup>( ~2.5kV/cm@30bar)
- Possibly add H<sub>2</sub>, N<sub>2</sub> or He to increase the drift velocity. (It will also reduce diffusion.)

been proposed and investigated. However, in the case of HPXe, the practical use on any particular gas mixture is restricted by the viability of employing the spark discharge technique for its purification. Because of this, the commonly used accelerating admixtures are H<sub>2</sub>, N<sub>2</sub> and recently He. A significant contribution in detailed studies of Xe mixtures with small percentages of H<sub>2</sub> and N<sub>2</sub> were carried by a group of MEPhI in the early 1980s [67, 91]. In these works, it was shown that H<sub>2</sub> is the most efficient drift accelerating agent among the practical admixtures.

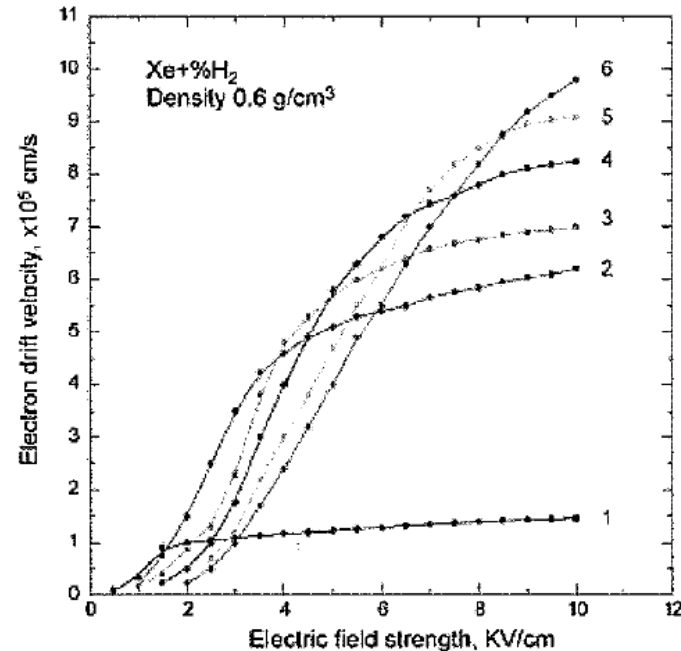


Fig. 3.3 Dependencies of electron drift velocities versus electric field strength in Xe+%H<sub>2</sub> mixture at 0.6 g cm<sup>-3</sup>. (1) - pure Xe, (2) - 0.2%, (3) - 0.3%, (4) - 0.5%, (5) - 0.7%, (6) - 1.0%. Redrawn from [91].

Admixture of helium to xenon also can be used for cooling and acceleration of drifting electrons. For example, at gas pressure 0.4 MPa admixture of 15% <sup>4</sup>He in xenon increases the electron drift velocity and reduces transverse diffusion about three times at reduced electric field of about  $3 \times 10^{-18}$  V cm<sup>-2</sup>

( $0.1 \text{ V cm}^{-1} \text{ Torr}^{-1}$  [93]. Similar observations were made at 2 MPa pressure and concentration of 13% <sup>4</sup>He [94] and 3% <sup>3</sup>He in xenon at reduced electric fields in the range of  $2-5.5 \times 10^{-18}$  V cm<sup>-2</sup> (results from A. Bolozdynya).

# Electrode for ionization mode

- In ionization mode, the Frisch grid is necessary.
  - Small pixel effect would not work for signal sum.
  - The intrinsic resolution has not been approached due to the high capacitance of the grid and its shielding inefficiencies. Such shielding grids are also notoriously sensitive to acoustic effects.

# Scintillation

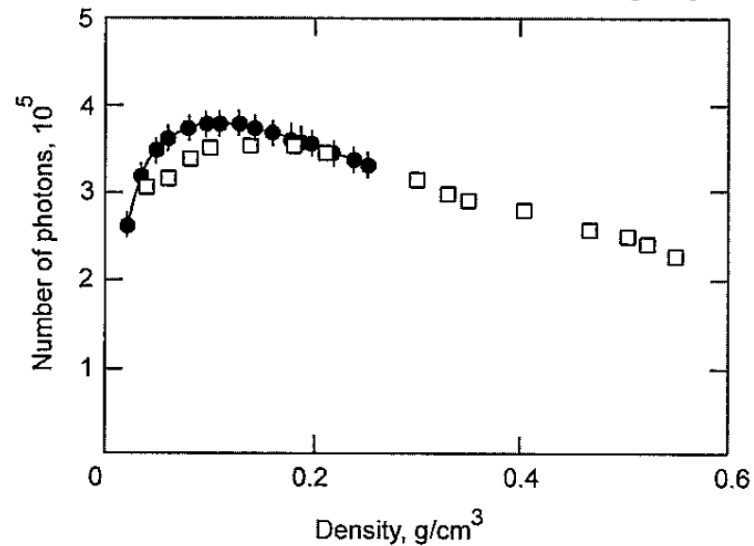


Fig. 3.38 Dependence of light output of scintillations excited by alpha particles on the density of high-pressure xenon: open squares represent data of Bolotnikov and Ramsey [33], closed circles represent data of Kobayashi et al. [198]. Redrawn from [198].

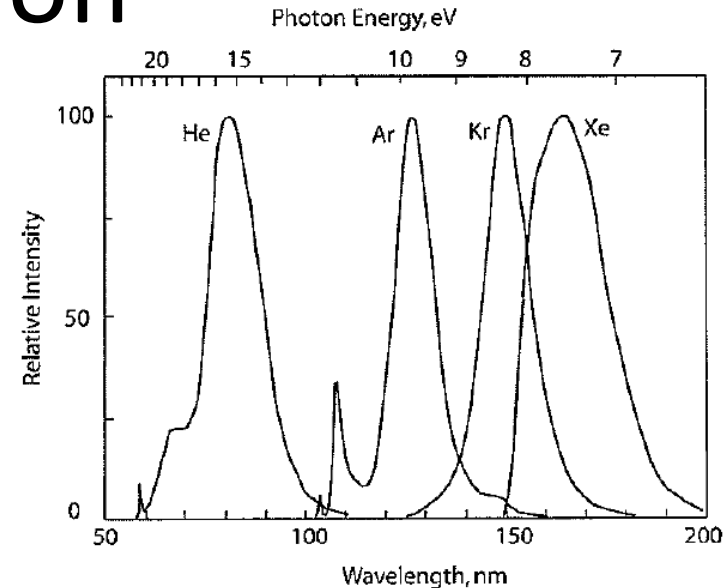


Fig. 3.27 Noble gas continua of helium, argon, krypton, and xenon normalized to the same intensity of the maximum. Redrawn from [176].

6. *Impurity emission.* Any impurity molecules present may quench the emission of hard UV light, and their own emission may be stimulated by transfer of excitation energy. This is of practical importance in the xenon, which is used as a wavelength-shifter the emission from helium or argon, which excitation energies are higher than the minimum xenon excitation level. At relative concentration of  $10^{-5}$ , nitrogen is adequate for efficient energy transfer from all the noble gases at atmospheric pressure. At relative concentration of  $10^{-3}$ , Xe can be used as a wavelength shifter, for example in  $^3\text{He}$  scintillator at 3.5 MPa pressure [171]. Sometimes, impurities have nonradiative transitions or emit in regions where the sensitivity of photodetectors is limited. This effect may dramatically reduce the observed light yield of noble gas scintillators.

What is the influence on scintillation from  $\text{N}_2$  or  $\text{H}_2$  addition?

# Electroluminescence

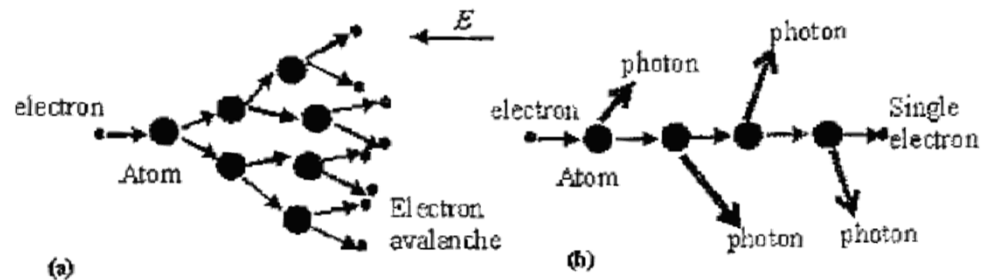


Fig. 6.2 Amplification process in gas detectors with gas gain (a) and electroluminescence (b) or proportional scintillation.

Good and stable linearity are expected because

- A linear amplification process.
  - c.f. Electron multiplication process is exponential process.
- The number of produced photons is proportional to the voltage drop rather than to the field strength.
  - Insensitive to the capacitance change by microphonic vibration

To keep original resolution determined by career generation,

- $\epsilon Y > 1/F$  ( $\epsilon > 5\%$  for 400 photons/e)
  - c.f. usually  $< 1\%$

# Photo-sensor

- VUV sensitive or using Wave-length-shifter.
- PMT
  - UV transparent window
    - Quartz, fused silica (=Synthetic silica?), CaF<sub>2</sub>?
- Photo-diode
  - Some of them are sensitive to VUV

# Wavelength shifter

**Tab. 4.1** High-pressure noble gas scintillation detectors.

	Pressure (MPa), size(cm)	WLS	Particle, Energy(MeV)	En. Res., % FWHM	Ref.
<sup>4</sup> He	13.8; 5 I.D.×8.6	7%Xe, DPS	n, 1.0	36	[234]
Ne	1.7	20%Xe	n, 3.5	6.7	[231]
<sup>3</sup> He	2.0	10%Xe	n, < 3	14	[232]
	3.5; 1.7×0.5	0.5%Xe, p-TP	n <sub>th</sub>	18	[171]
	24.8; 38 cm <sup>3</sup>	DPS	n <sub>th</sub>	54	[233]
			α, 5.15	16	
	20.0; 4 I.D.×4	5%Xe, p-TP	n, 2.5	4.8	[236]
	13.8; 5 I.D.×8.6	2%Xe, DPS	n <sub>th</sub>	31	[235]
Xe	2.8	25%N <sub>2</sub>	n, 0.5	29.5	[231]

Note: WLS - wavelength shifting; DPS - trans p,p'-diphenylstilbene; p-TP - paraterphenyl; n<sub>th</sub> - thermal neutrons.

- Acrylic tube coated with a thin layer of polysterene doped with organic fluor TPB ( tetraphenyl butadiene) (p.114)
- N<sub>2</sub> output peak 340nm

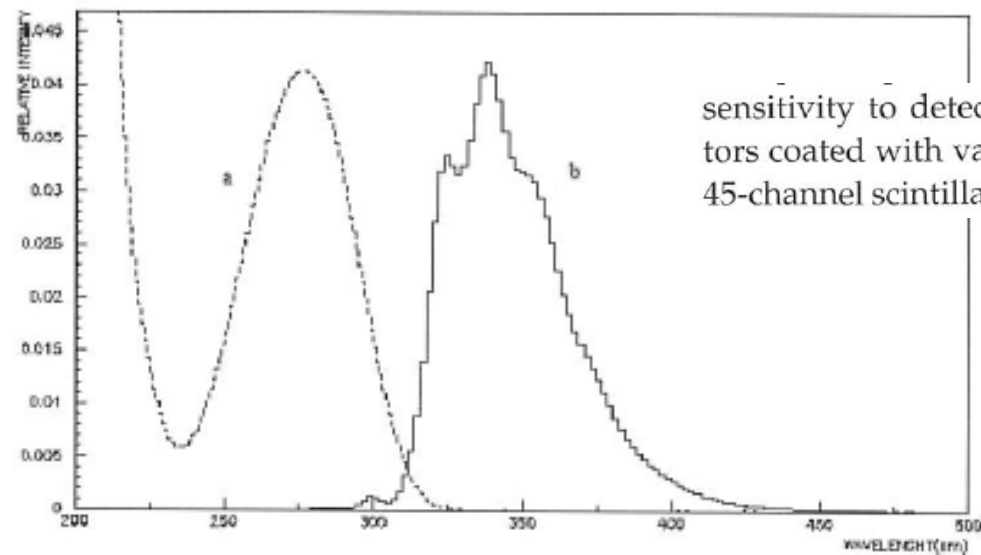
### 8.5.2.1 Wavelength Shifters Dissolved in Noble Gases

One of the first wavelength shifters used with noble gas scintillators was a gas admixture of nitrogen. For example, Grün and Schopper [228] used argon in mixture with 2% of nitrogen in their development of a detector for triggering of cloud chambers. The addition of a small amount of nitrogen to noble gases enhances the light emission in the blue range. At earlier studies it was concluded that nitrogen acts as a simple fluorescent converter. However, the nitrogen also acts as the quenching agent: its addition to the noble gas results in decreasing the absolute scintillation efficiency. For example, Northrop and Nobles [13] observed that there is a reduction in the practical light output of a xenon gas scintillator, used with solid wavelength shifter, when nitrogen is added. The efficiency is reduced by about 1/3 by addition of 10% of nitrogen or hydrogen. The latter is often used in high-pressure xenon detectors to increase the drift velocity of electrons. Another undesirable feature of nitrogen is the introduction of a slower component of decay time. For example, the addition of  $10^{-4}$  N<sub>2</sub> introduces in argon scintillator a component with decay time of 0.5  $\mu$ s, which accounts for 75% of the total photon emission [170]; the decay time reduces with an increase in the concentration of nitrogen, however, this reduces the total light yield. From all these facts, one can conclude



### 8.5.2.2 Solid Wavelength Shifters

A number of solid wavelength shifters deposited onto optical elements such as windows and mirrors have been considered including *trans*-stilbene, tetraphenylbutadiene (TPB), sodium salicylate, p-quaterphenyl, diphenylstilbene, and p-terphenyl (see, for example, McKinsey et al. [429] and references therein). The last one was found to be the best one to be used with xenon and xenon-containing gas mixtures from the point of view of high quantum efficiency ( $> 90\%$  according to Belogurov et al. [144]), low hygroscopic, chemical inertness, and exclusive radiation hardness. Emission and absorption spectra of p-terphenyl are presented in Fig. 8.10.



sensitivity to detection of Cherenkov light [431]. Aluminized Mylar reflectors coated with vacuum deposited p-TP have been used in construction of a 45-channel scintillation LXe/LKr electromagnetic calorimeter (see Chapter 4).

**Fig. 8.10** (a) Absorption and (b) emission spectra of p-terphenyl [407].

The p-terphenyl is reported to have a short decay time of 2–5 ns and widely used as a scintillating dye in plastic scintillators. Kumar and Datta [430] com-

# Wavelength shifter – *p*-terphenyl

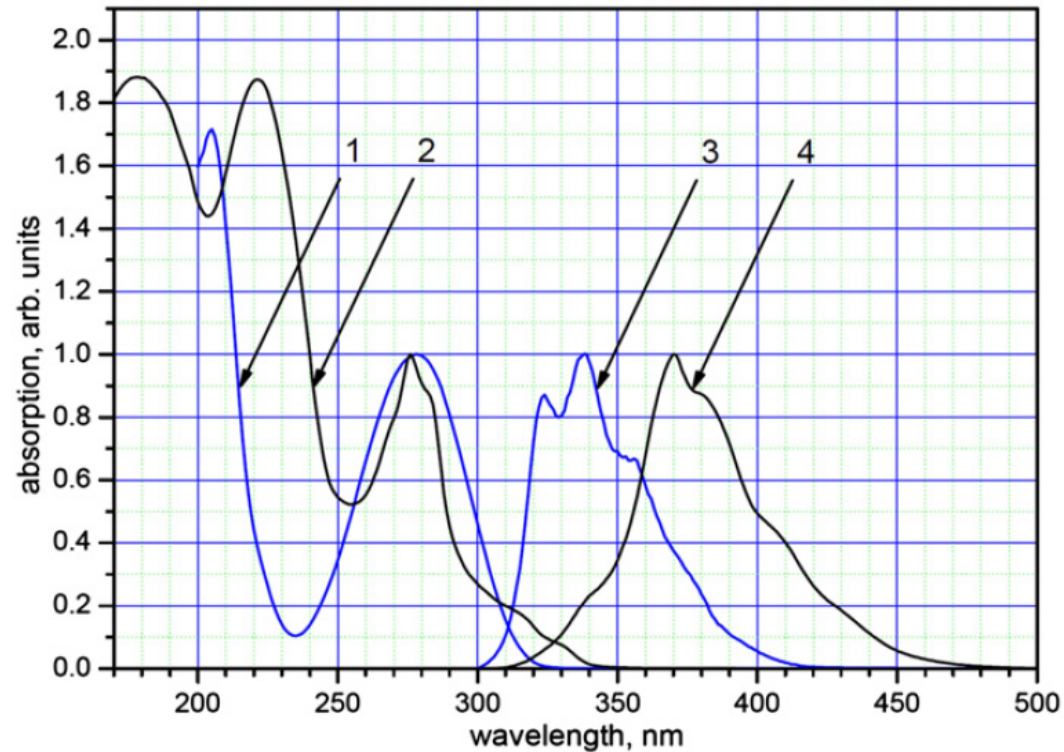


**Fig. 1.** Absorption and emission spectra of *p*-terphenyl. 1 – *p*-terphenyl in solvent, absorption, 2 – polycrystalline *p*-terphenyl, absorption, 3 – *p*-terphenyl in solvent, emission, 4 – polycrystalline *p*-terphenyl, emission.

D.Yu.Akimov et. al, “Development of VUV wavelength shifter for the use with a visible light photodetector in noble gas filled detectors”

<http://dx.doi.org/10.1016/j.nima.2011.12.036>

## 8.5

### UV Light Collection

#### 8.5.1

##### Reflectors

The best broad band reflectance properties in the extreme UV range have been demonstrated with metal (aluminum, iridium, gold, rhodium, platinum) coatings *enforced* with  $\text{MgF}_2$ . The reflectance of such mirrors may achieve 90% in the range from 400 nm down to  $\sim 160$  nm. There are many different base materials used for metal reflectors and ranged from optical glasses to polymer films such as Mylar. For example, aluminized Mylar has been used for production of multicell reflecting structures of LKr and LXe scintillation calorimeters [190,361]. Specially designed multilayer dielectric coatings, consisting of alternating quarter-wavelength layers of high and low refractive index media on high-quality optical substrate, offer up to 99% reflectance for certain wavelengths such as 157 nm and 193 nm in the narrow ( $\pm 5$  nm) band used in optical systems of excimer lasers. There are commercially available polymer films with multilayer dielectric coating that provides high reflectivity in a broad band of visible range. For example, Vikuiti<sup>TM</sup> Enhanced Specular Reflector (ESR) is used as a highly efficient light guide or bulb cavity reflector with a reflectivity of 98.5% across the visible spectrum.

The diffuse reflectance of pressed PTFE (polytetrafluoroethylene) powder is very high over the spectral range of 220–2500 nm [426,427]. The reflectance of PTFE powder is influenced by the density to which the powder is pressed. The highest reflectance in the range 300–1800 nm is achieved at  $1.0 \text{ g cm}^{-3}$  density and it drops for 2% at density of  $2 \text{ g cm}^{-3}$ , which is standard for bulk construction Teflon. Similar diffuse reflectance properties have been demonstrated with *Spectralon* by Labsphere. *Spectralon* is a thermoplastic resin that can be machined in a variety of shapes for the construction of optical components. The material has a hardness roughly equal to that of high-density polyethylene and is thermally stable up to 623 K. The manufacturer states that *Spectralon* gives the highest diffusible reflectance of any known material or coating over the UV-VIS-NIR region. Space-grade *Spectralon* is extremely pure and low outgassing.

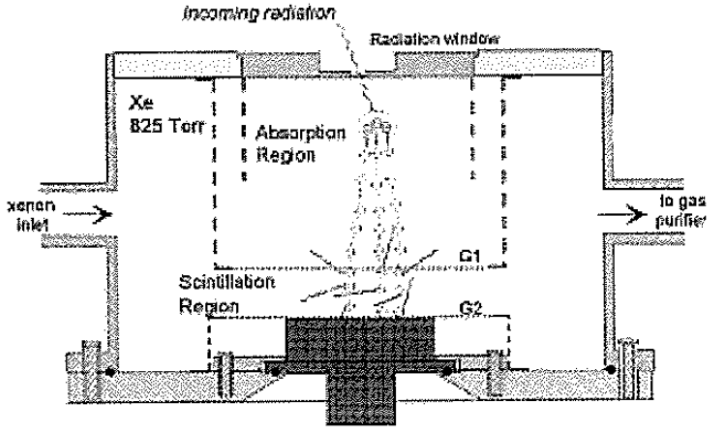
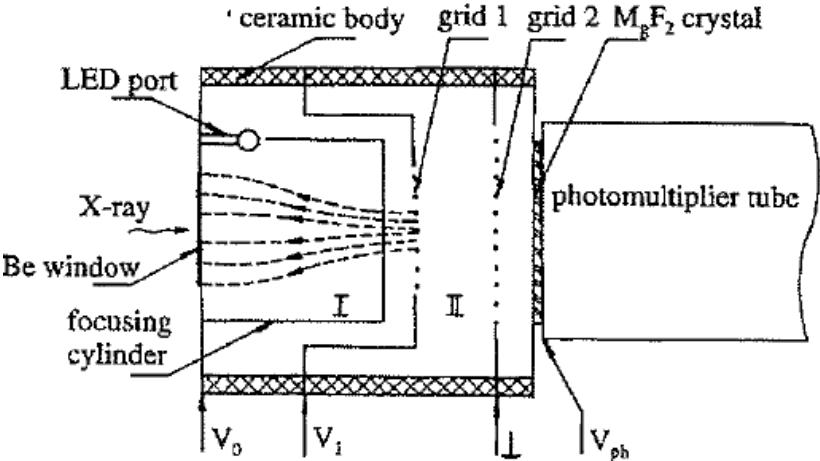
Optical properties of selected diffuse reflective materials have been studied in the 120–220 nm range by Kadkhoda et al. [428]. They found that *Spectralon* and PTEF exhibit a high reflectance ( $> 70\%$  and  $> 55\%$ , respectively) and Lambertian scatter behavior for the spectral region above 175 nm, but no significant reflectance is observed for these materials below 170 nm. With respect to the stability of its optical properties, PTEF is not recommended for applications below 220 nm. Microroughened SiC ceramic shows a Lambertian scatter behavior for the entire spectral region from 120 nm to 220 nm with

# reflector

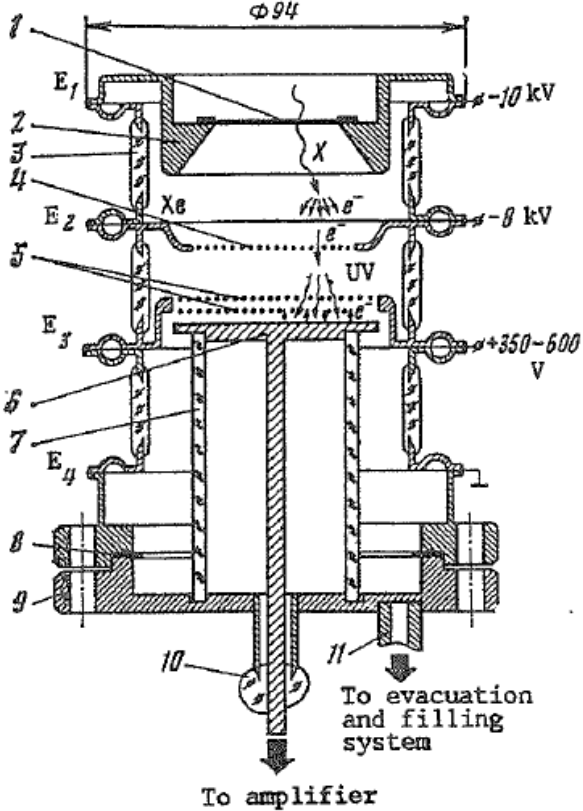
reflectance about 20% above 160 nm. The reflectance factor of SiC can be enhanced with the help of a high reflective thin metal coating. Similar properties are demonstrated by  $\text{BaSO}_4$ .

It is interesting to note that there is data demonstrating that PTFE works as a weak wavelength shifter with excitation band in the range of  $< 290$  nm and emission band in the wavelength range of 310–350 nm [426]. This observation may explain why PTFE reflectors have been successfully used in LXe scintillation detectors equipped with photomultipliers with low quantum efficiency below 180 nm [245].

# Gas Proportional Scintillation Counters



Large(16mm diameter) Area Avalanche Photodiode (LAAPD) by Photonics



Open photocathode(e.g. CsI) readout

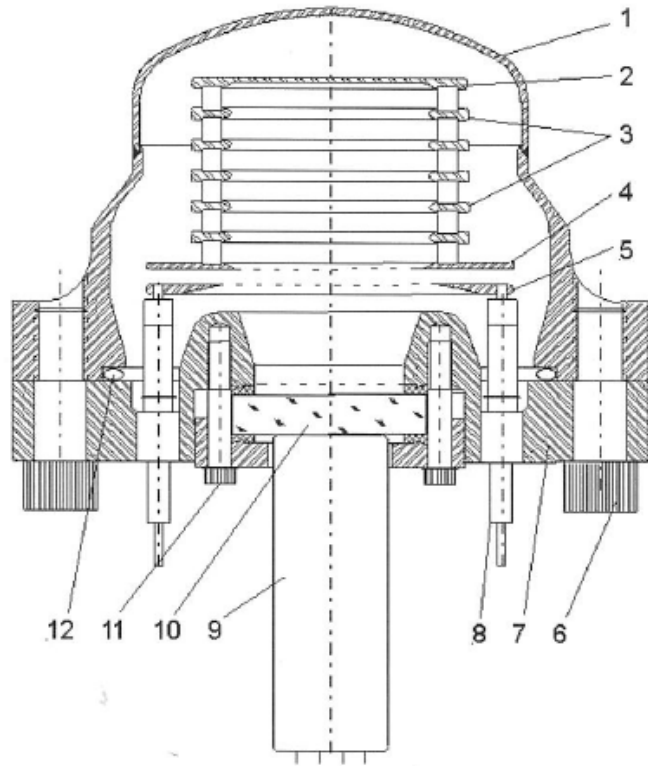


**Fig. 6.13** Electroluminescence high-pressure xenon detector with parallel plate electrode system and photomultiplier readout. Note: 1 - high-pressure vessel; 2 - aluminum cathode; 3 - drift electrodes separated by stand-off ceramic insulators; 4 and 5 - grid electrodes forming electroluminescence region; 6 - bolt; 7 - flange; 8 - HV feedthroughs; 9 - photomultiplier; 10 - optical window coated with p-terphenyl wave-length shifter; 11 - bolt; 12 - Helicoflex gasket in aluminum jacket. Sensitive volume of the detector enclosed into the electrode system of 2-4 has a 5-cm diameter and 5-cm depth [312].

A  $0.5 \text{ mg cm}^{-2}$  layer of p-terphenyl ( $\text{C}_{14}\text{H}_{18}$ ), serving as a wave shifter, was vacuum-deposited on the input surface of the optical window, enabling the photomultiplier to see the 170 nm UV light generated during the electroluminescence process. The quantum efficiency of the p-terphenyl wave shifter has been measured to be  $> 90\%$  in pressurized xenon [144]. The emission spectrum of p-terphenyl has 2 peaks: one at 350 and another at 450 nm. An important property of this well-known scintillating dye is that it does not contaminate xenon. High voltage feedthroughs (8) were installed in the flange

Before assembly, all metal and ceramic-made detector parts were baked at 500 K under a vacuum of  $< 10^{-4}$  Pa. The assembled detector was pumped down to  $10^{-6}$  Pa for a week before filling with xenon. Pure Xe or Xe+0.2% $\text{H}_2$  gas mixture used to fill the detector. A spark purification technique was used to remove electronegative impurities from the gas. The ultimate purity of the gases used in these investigations corresponded to several milliseconds of electron lifetime.

The detector operates in the following manner. Ionization radiation absorbed in the sensitive volume generates electrons, which drift into the EL region and generate an EL flash. UV light is shifted into the 350–450 nm range by p-terphenyl deposited on the inside surface of the window viewed by the PMT.

The EL detector was tested with pure Xe and Xe+0.2% $\text{H}_2$  gas mixtures pressurized up to 3.1 MPa. The best energy resolution was achieved at pressures of about 2 MPa. In order to prove the statement about vibration insensitivity, an electric engraver (10 W, 60 Hz) was used to disturb the ELD. The writing pin of the engraver was installed onto the flange of the ELD. Pulse height spectra of  $^{241}\text{Am}$  gamma source were taken for the same acquisition time while the engraver was working and when it was turned off. No significant difference between spectra in the range of  $>10$  keV was found (Fig. 6.14).

When repeated with HPXe ionization chambers, the test demonstrated that the working engraver generated enormous signals exceeding the ionization signals from the gamma sources by two orders of magnitude, i.e., the microphonic effect introduces the risk of damage to preamplifiers and prohibits any spectral measurements with HPXe detectors under these conditions.

In attempt to construct a more robust HP ELD, the fragile optical window and PMT in the detector described above detector were replaced with a large avalanche photodiode installed directly inside the detector [328]. The input surface of the LAAPD was coated with p-terphenyl wavelength shifter. The detector demonstrated about the same energy resolution as it did using a PMT readout, however, it was found to be more sensitive to vibrations because of vibrosensitivity of the used charge-sensitive preamplifier that was installed directly onto the flange of the detector. The authors planned potting preamplifier with GE RTV in order to reduce the vibration of the wiring.

One of the most successful SDCs (Fig. 6.19) consists of a stainless steel pressure vessel and an electrode structure, supporting a 37-mm deep drift region followed by a 6-mm deep light-generating gap defined by two wire electrodes. Scintillations in the drift region and electroluminescence in the light-generating gap were both detected by nineteen 80-mm diameter glass photo-multipliers (PMTs). Each PMT was optically coupled to a separate glass window, the inside surface of which was covered by a p-terphenyl wave shifter. A 3-mm thick spherical aluminum entrance window allows gas pressure of up to 2 MPa. An additional grounded thin aluminum electrode is installed to maintain a uniform electric field in the drift region. Radiation absorbed in the drift region produces primary scintillations in addition to ionization clusters. In the low reduced electric field ( $\sim 0.1 \text{ kV cm}^{-1} \text{ bar}$ ) applied to the drift region, the electron clusters drift to the light-generating gap, where the high reduced electric field ( $2\text{--}3 \text{ kV cm}^{-1} \text{ bar}$ ) is applied to generate electroluminescence of the gas. The two-dimensional position of the point-like ionization clusters projected on the light-generating gap is measured from the distribution of the electroluminescent signals over the PMT array. The coordinates and

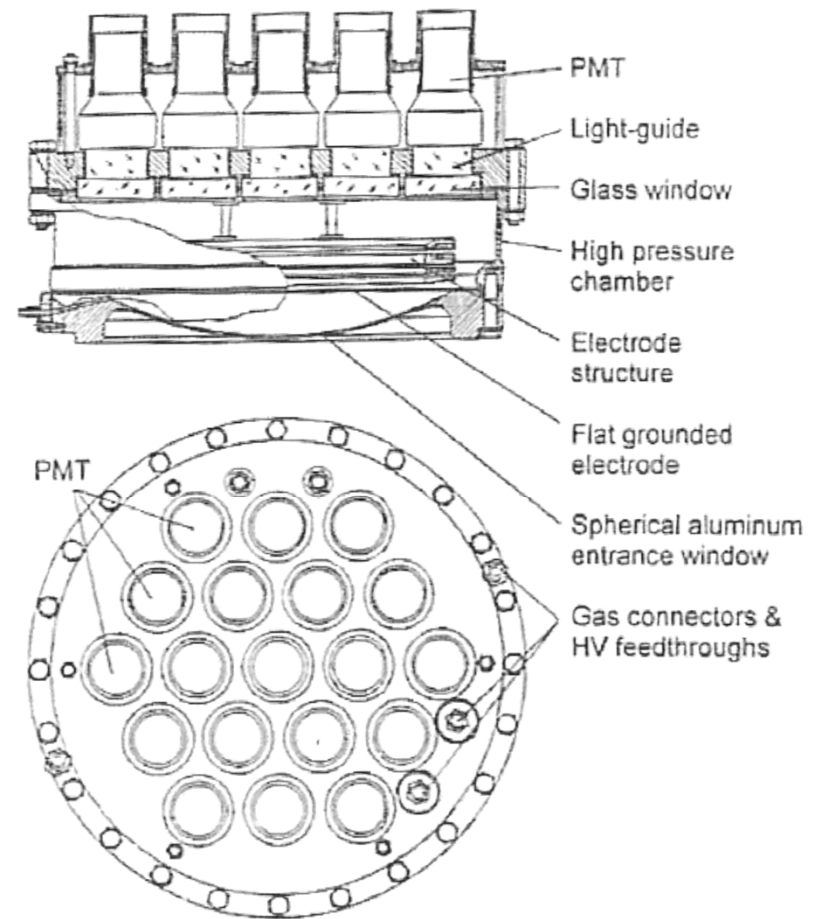
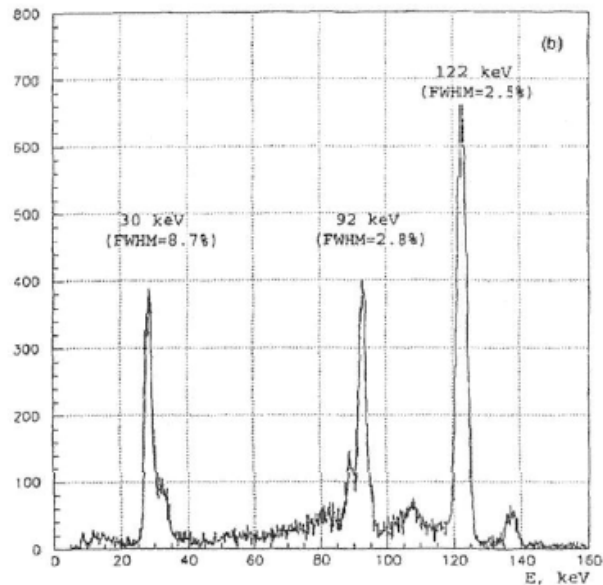


Fig. 6.19 Schematic diagram of the scintillation drift chamber SDC-19.



@0.9MPa

Fig. 6.21 Pulse height distributions measured: (a) for  $^{241}\text{Am}$  and (b)  $^{57}\text{Co}$  gamma rays sources from the scintillation drift chamber SDC-19 [304].

# Gas purification

MEG prototype

ameter) tungsten wires suspended inside the detector volume. Xenon is continuously evaporated, passed through an Oxisorb cartridge, a molecular sieve and a hot metal getter and condensed back in the detector. During several weeks of operation, the absorption length of scintillation light was increasing and has reached  $>150$  cm in four weeks. Mass-spectrometric analysis has shown the presence of water as a dominant impurity in xenon. Monte Carlo

# Spatial resolution



# End point blob

## 2.4.3

### Influence of $\delta$ -Electrons

$= 12 \pm 3 \text{ kV cm}^{-1}$ . As it was shown in [57], there are a few tens of  $\delta$ -electrons of 1–20 keV energy generated along the beta particle track; on average, 10 to 20% of the absorbed energy is deposited in  $\delta$ -electrons. Statistical fluctuations in the number of generated  $\delta$ -electrons may significantly affect the energy resolution of liquid xenon ionization chambers.

Need simulation study.

A.I.Bolozdynya and V.L.Morgunov,  
IEEE Trans. Nucl.Sci. 45, 1646-

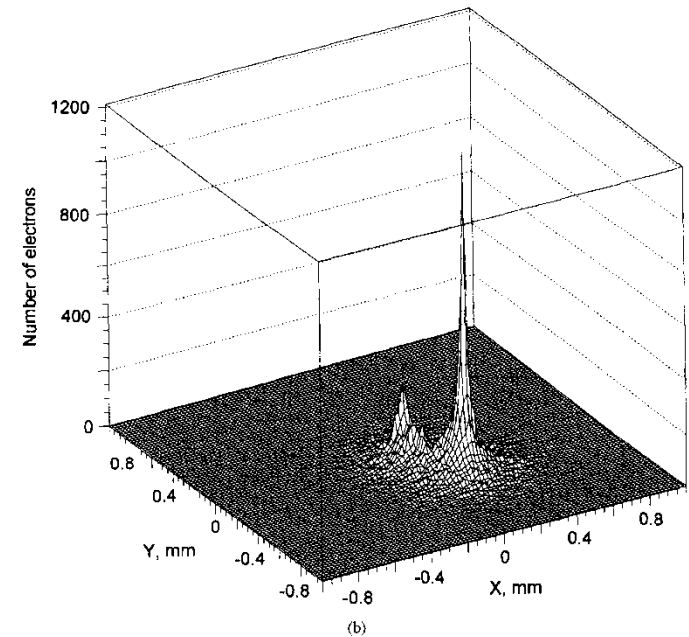
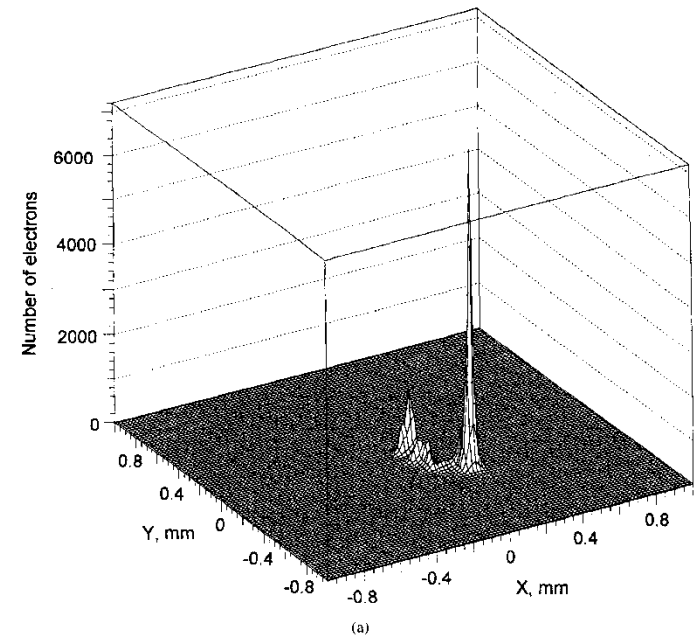


Fig. 3. (a) Distribution of secondary ionization electrons in the original 50-keV ionization cluster and (b) in the same cluster after 800-ns drift-time at electric field of 2-kV/cm-bar in 20-bar Ar.

# Readout by light collection cell (Maybe new idea?)

